Analysis of the Neuron-specific IIS/FOXO Transcriptome in Aged Animals Reveals Regulators of Neuronal and Cognitive Aging

Yifei Weng[1], Shiyi Zhou[1], Katherine Morillo[1], Rachel Kaletsky[1,2], Sarah Lin[1], and Coleen T. Murphy[1,2]*

[1]Department of Molecular Biology, Princeton University, Princeton, NJ 08544, USA

[2]Lewis Sigler Institute for Integrative Genomics, Princeton University, Princeton, NJ 08544, USA

*Corresponding author: ctmurphy@princeton.edu

Summary

Cognitive decline is a significant public health concern in our aging society. In this study, we used the model organism *C. elegans* to investigate the impact of the IIS/FOXO pathway on age-related cognitive decline. The daf-2 Insulin/IGF-1 receptor mutant exhibits a significant extension of learning and memory span with age compared to wild-type worms, an effect that is dependent on the DAF-16 transcription factor. To determine the mechanisms by which aging *daf-2* mutants can maintain learning and memory with age while wild-type worms lose neuronal function, we carried out neuron-specific transcriptomic analysis in aged animals. We observed downregulation of neuronal genes and upregulation of transcriptional regulation genes in aging wild-type neurons. By contrast, IIS/FOXO pathway mutants exhibit distinct neuronal transcriptomic alterations in response to cognitive aging, including upregulation of stress response genes and downregulation of specific insulin signaling genes. We tested the roles of significantly transcriptionally-changed genes in regulating cognitive functions, identifying several novel regulators of learning and memory. These findings suggest a potential mechanism for regulating cognitive function with age and offer insights into novel therapeutic targets for age-related cognitive decline.

Introduction

Learning and memory loss have become prevailing problems in our aging society. In a 2008 study, it was found that at least 22.2% (about 5.4 million) individuals over the age of 71 in the United States have at least mild cognitive impairment[1–3]. Furthermore, global dementia cases are predicted to triple from an estimated 57.4 million cases in 2019 to 152.8 million cases in 2050[4,5]. As most industrialized countries are experiencing a rapid increase in the proportion of the aged population, understanding and potentially preventing the underlying issues of neuronal structural and behavioral decline associated with aging is crucial for societal health.

C. elegans is an excellent model system for studying neuronal aging, given its tractable genetics, short lifespan, simple nervous system[6], and rapid loss of learning and memory with age[7]. In addition, many human neuronal aging phenotypes and genes of interest for healthcare solutions are conserved in *C. elegans*[8], making discoveries in *C. elegans* possibly applicable to humans.

The Insulin/IGF-1 like (IIS)/FOXO pathway was first discovered to play a role in longevity in *C. elegans*. The lifespan of *daf-*

2/IIS receptor mutants is twice that of wild-type animals, and this lifespan extension requires the downstream Forkhead box O (FOXO) transcription factor DAF-16[9]. DAF-16/FOXO controls the expression of various genes, including stress response, proteostasis, autophagy, antimicrobial, and metabolic genes[10]. As a conserved regulator, the IIS/FOXO pathway also regulates longevity in Drosophila, mice, and humans[11–14].

In addition to regulating lifespan, the IIS pathway regulates neuronal function via the FOXO transcription factor. In particular, *C. elegans* IIS/*daf-2* mutants display DAF-16-dependent improved learning, short-term memory, and long-term memory[7]. To further investigate the role of the neuronal IIS/FOXO pathway, we previously performed neuron-specific RNA-sequencing in young adult *C. elegans* and identified neuron-specific targets[15]; genes upregulated in *daf-2* mutant neurons are distinct from those in the whole animal, and we found that these neuronal genes are necessary for the observed improvements in memory and axon regeneration in *daf-2* mutant worms.

While both young and old *daf-2* adult worms have improved learning and memory, the mechanism by which *daf-2* mutants maintain neuronal function in older worms is not yet understood. Compared to wild-type worms, *daf-2* mutants maintain maximum velocity[16], neuromuscular junctions, motility[17,18], and neuronal morphology better with age[19–21], and maintain the ability to regenerate axons in aged animals[22,23]. Previously, we found that *daf-2* worms also extend learning beyond wild-type's ability[7], but the full duration of this extension was not known. Here we find that the learning and memory ability of *daf-2* worms is extended with age to a greater proportion than its lifespan extension effect. To determine the transcriptional differences in the aging nervous system that might contribute to the loss of neuronal function with age in wild-type worms and the differences responsible for the extended abilities of *daf-2* animals, we transcriptionally profiled aged wild-type and IIS/FOXO mutants. We then used functional assays to assess their contributions to learning and memory; genes expressed at higher levels in aged wild-type neurons impair learning and memory, while *daf*-2's neuronal targets in older worms are required to maintain neuronal functions with age.

Results

Neurons lose their neuronal function and identity with age

Previously, we found that cognitive abilities in *C. elegans,* including learning, short-term memory, and long-term memory, all decline with age[7]. Moreover, neuronal morphology and regeneration ability are also impaired with age[19–22]. However, how these phenotypes are regulated at the molecular level in aging neurons remains to be systematically characterized. Therefore, we were interested in identifying gene expression changes with age in neurons to characterize the normal physiological aging process.

Adult Day 1 worms are fully developed, young, and healthy, while Day 7-8 worms, although still in their mid-life, have completely lost their learning (**Figure 1A**) and memory (**Figure 1B**) abilities[7]. This decline in behavior resonates with the morphology decline with age in the AWC neurons (**Figure 1C**), which are required for our associative learning and memory formation[24]. We found that neurite beading (**Figure 1D**) and wavy processes (**Figure 1E**) increase with age in the AWC neurons, which may affect synaptic connectivity and signal transduction, leading to dysfunction and learning and memory impairments.

To identify genes that regulate age-related morphological and functional decline in wild-type neurons, we performed neuron-specific transcriptomic analysis on six

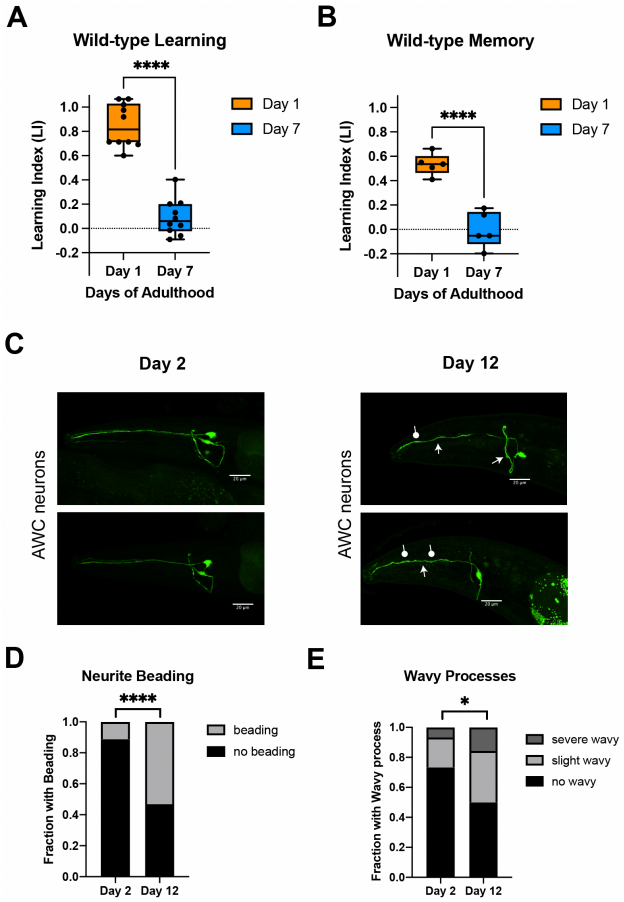

Figure 1. Aging causes behavioral and morphological changes in worm neurons. (A-B) Day 1 and Day 7 Learning (A) and memory (B) in wild-type N2 worms, N = 5. (C) Representative images of Day 2 and Day 12 AWC neurons. Arrow: neurite deviation. Round arrow: beading. (D) Quantification of neurite beading with age. Chi-square test, p <0.0001. (E) Quantification of neurite deviation with age. Chi-square test, p = 0.0471.

replicates of FACS-isolated neurons from Day 1 and Day 8 adult wild-type worms (**Figures S1 A, B**). Because we previously found that whole-worm analyses mask changes found specifically in the neurons[15], to complement our aging neuron studies, we also carried out analyses of aging whole worms (**Figure S2A-E, Table S1**), which is dominated by changes in the extracellular matrix (**Figure S2B**), stress response/ pathogen genes (**Figure S2C**) and the alimentary system (intestine) (**Figure S2D**), overshadowing neuronal changes. Principal components analysis of the neuron RNA-seq samples indicated that they are well separated by age (**Figure 2A**), and downsampling analysis[25] suggested that we sequenced to saturation (**Figure S1E**), with an average of 41,636,463 uniquely counted reads, and we detected the expression of 19,725 coding and non-coding genes ($\log_{10}$(TPM)>0.5) (**Figure S1C**).

We performed differential expression analysis to find neuronal genes that change with age (**Figure 2B, Table S2**). Tissue enrichment analysis suggested that neuronal sorting and sequencing was successful, and that aging neurons lose genes most expressed in the nervous system and neurons (**Figure 2C**). Gene ontology (GO) analysis suggested that genes declining with age in neurons encode for proteins important in neuronal function (**Figure 2D**) , including synaptic proteins (e.g., *srh-59, rab-3, sng-1, sup-1*), potassium channels (e.g., *egl-23*, *twk-7*, *twk-49*, *ncs-5*), and transmembrane transporters (e.g., *folt-2, ccb-2, unc-79, exp-1*). The decrease in ex-pression of these genes during aging may indicate that neurons are losing their identity and their ability to perform neuronal functions, such as signal transduction and axonal transport, and correlates with the behavioral and morphological declines observed in aging wild-type worms. Comparing whole-worm sequencing and neuron-specific sequencing, we found that genes involved in metabolic processes, structural proteins, lipid localization, and muscle system processes decline with age in the body, while neuron-specific sequencing loses synaptic proteins, neuropeptide signaling, and other neuron functions (**Figure 2E**). Neurons could be overshadowed in the whole-worm transcriptome, suggesting that studying these unique neuronal age-related changes could reveal novel mechanisms of cognitive aging.

Many genes that are more highly expressed in young neurons are known to be specific to a subset of neurons. For example, *ins-6*, an insulin-like peptide specific to the ASI, ASJ,

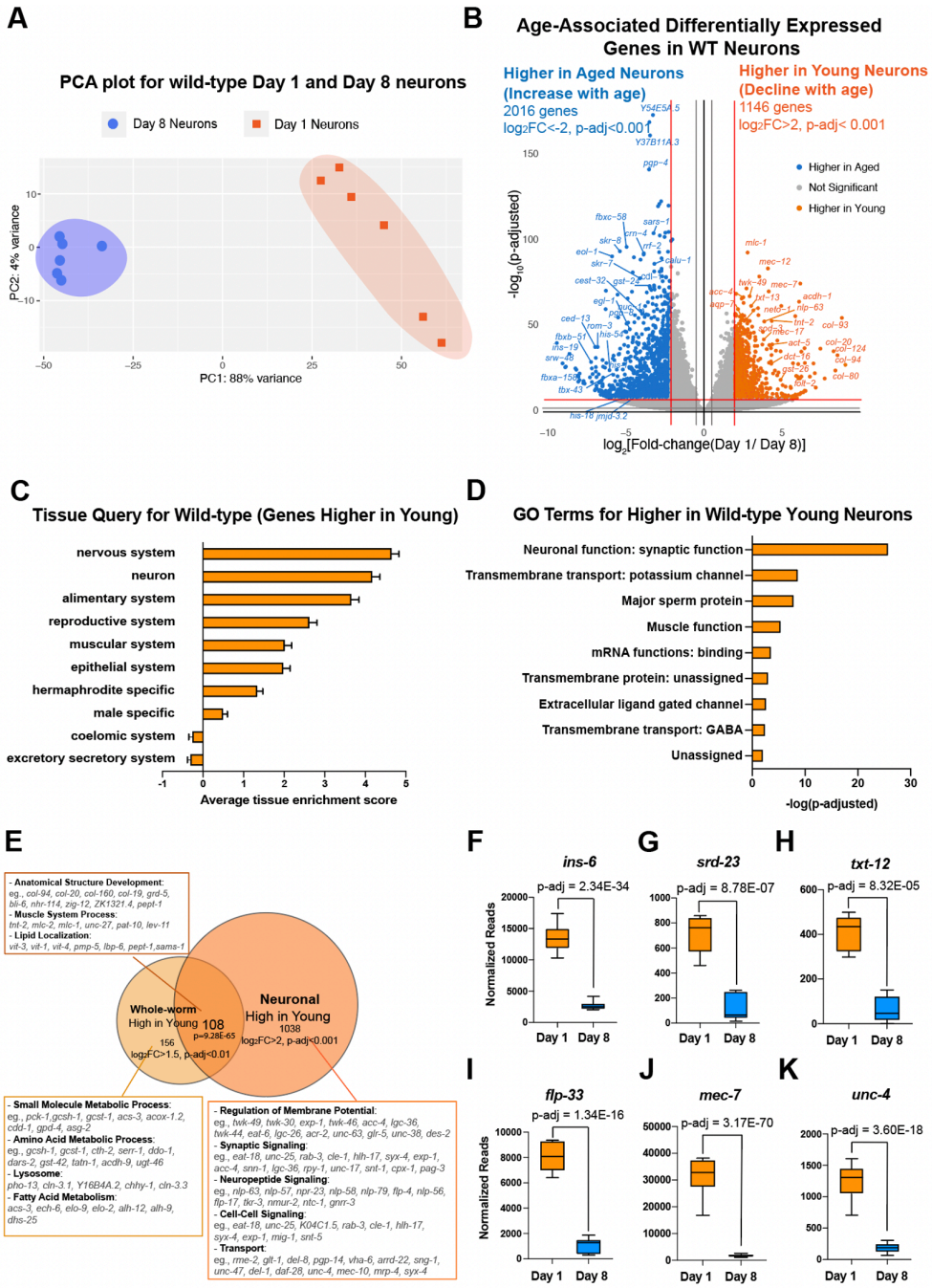

Figure 2. Identifying neuronal aging targets in WT worms using neuron-specific RNA-sequencing. (A) PCA plot for Day 1 (orange) and Day 8 (blue) neuronal bulk RNA-seq samples. (B) Volcano plot comparing age-associated differentially-expressed genes in WT neurons. Genes downregulated with age (orange) and upregulated with age (blue) were obtained by neuron-specific RNA sequencing of adult wild-type animals with neuron-specific GFP expression. (Adjusted p-value < 0.001, $\log_2$(Fold-change) > 2. N = 6 biological replicates per age. 1146 genes were significantly downregulated with age (higher in young neurons) and 2016 genes were upregulated with age (higher in old neurons) (C) Tissue prediction scores for genes higher in young neurons. Nervous system and neurons have the highest prediction score. (D) GO terms of genes that decline with age in wild-type neurons. Synaptic and signaling GO terms enriched in neuronal genes p-value calculated using hypergeometric distribution probability. (e) Comparison of whole-body higher-in-young genes and neuronal higher-in-young genes. GO Terms and representative genes were performed using g:Profiler software. P-value of overlapping regions were calculated using a hypergeometric calculator. (f-k) Normalized reads of *ins-6, srd-23*, *txt-12*, *flp-33*, *mec-7*, *and unc-4* in Day 1 and Day 8 neurons in our dataset. P-adjusted values were calculated from DESeq2 software.

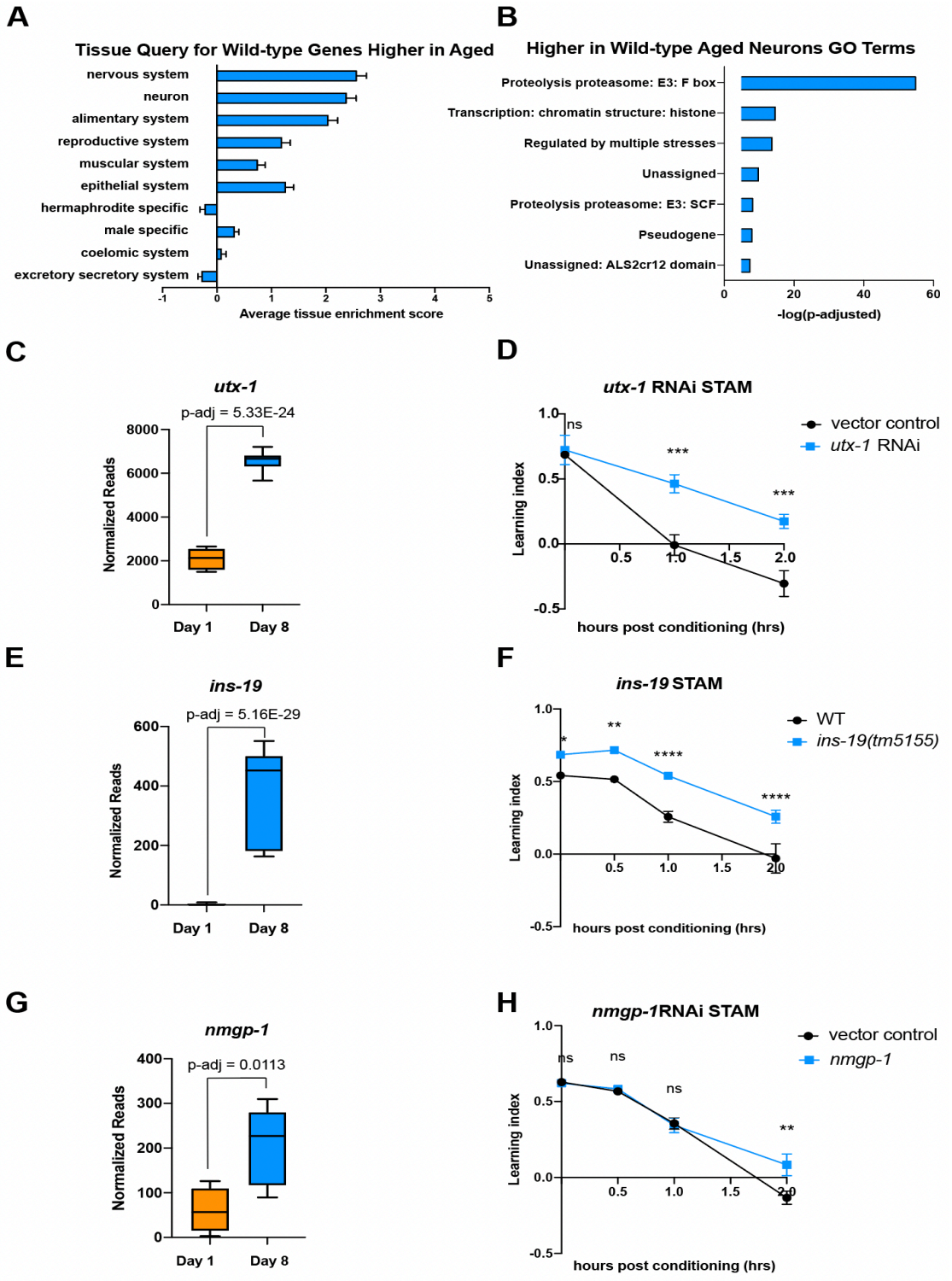

Figure 3. Genes that increase with age cause behavioral defects. (A) Tissue Query for wild-type genes expressed at higher levels in aged worms show lower neuron-specific prediction score. (B) GO terms of genes expressed higher in aged neurons highlight transcription regulation and proteolysis. GO term analysis was done using Wormcat 2.0 (Holdorf et al. 2020). (C) Normalized reads of *utx-1* on Day 1 and Day 8. (D) Short-term associative memory (STAM) assay shows that adult-only *utx-1* knockdown improves 1hr and 2hr memory of wild-type worms on Day 2. (E) Normalized reads of *ins-19* on Day 1 and Day 8. (F) *ins-19* mutation improves learning and memory in STAM on Day 3 of adulthood. (G) Normalized reads of *nmgp-1* on Day 1 and Day 8. (H) *nmgp-1* RNAi knockdown improves memory in STAM on Day 2. P-adj value of normalized count change generated from DEseq2 analysis. N = 5 plates in each behavioral experiment. Representative result of 3 biological repeats is shown. *: p<0.05. **: p<0.01. ***: p<0.001. ****: p<0.0001

and AWA neurons[26] that regulates longevity[27] and aversive learning[28], is significantly downregulated with age (**Figure 2F**). *srd-23*, a serpentine receptor located at the AWB neuron cilia[29], also decreases in expression with age (**Figure 2G**). Furthermore, various genes specific to some sensory neurons (**Figure 2H, I**) touch neurons (**Figure 2J**), and motor neurons (**Figure 2K**) decline in expression with age. The decreased expression of these neuron-type-specific genes with age may impact the function of individual neurons and disrupt neural circuit communication, ultimately contributing to the declines in behavior observed with age.

As neurons age, genes that increase in expression, while assigned to the nervous system (**Figure 3A**), are less specific for neuron function; instead, aged wild-type neurons express higher levels of many predicted F-box genes with predicted proteasome E3 activity (e.g., F-box proteins *fbxa-158*, *fbxb-51*, *pes-2.1*, and SKp1-related proteins *skr-12*, *skr-6*). Some transcription regulation (e.g., *ced-13, tbx-43, nhr-221,* and *end-1*), and chromatin structure/function (e.g., *his-54, dot-1.2, jmjd-3.2, hil-7,* and *utx-1*) genes also increase with age (**Figure 3B**), although neurons appear to lose their neuron-specific transcriptional identity with age.

We hypothesized that genes that are expressed at higher levels in aged neurons might be harmful to neurons, and therefore reducing their expression might be beneficial to the worm. To investigate this hypothesis, we tested the candidates *utx-1* (a histone demethylase known to play a role in development[30] and lifespan in worms[31–33], whose homolog has been implicated in cognition in mammals[34,35]), *ins-19,* an insulin-like peptide, and *nmgp-1*, a neuronal glycoprotein involved in chemosensation[36] (**Figure 3C, E, G**). We found that adult-only knockdown of *utx-1* increases 1hr and 2hr memory (**Figure 3D**), mutation of *ins-19* increases both learning and memory (**Figure 3F**). and the adult-only knockdown of *nmgp-1* extends memory at 2 hours (**Figure 3H**). These results indicate that neuronal genes that increase with age can have a negative impact on learning and memory.

Aging IIS/FOXO neurons express stress-resistance genes

Not only do young *daf-2* worms have better memory than wild-type worms, but *daf-2* mutants also maintain learning and memory better with age[7,15]. We found that while wild-type worms lose their learning and short-term memory abilities by Day 7 (**Figure 1A**), learning and memory span were significantly extended in *daf-2* mutants (**Figure 4A**), and this extension is dependent on the FOXO transcription factor DAF-16 (**Figure 4A**). *daf-2* worms maintained learning ability until Day 19 and short-term (1hr) memory ability until Day 15 (**Figure 4B**), more than twice the duration of wild-type worms, while *daf-16;daf-2* worms exhibit no short-term memory ability, even on Day 1 of adulthood. Previously, Bansal et al. (2105) suggested that despite having a longer lifespan, *daf-2* mutants have worse proportional health span and extended "end-of-life misery"[37]; however, our data suggest that the learning span and memory span-to-lifespan ratios in *daf-2* worms are slightly higher than that of wild-type worms (**Figures 4C, D**), indicating that *daf-2* mutants maintain cognitive function for a longer proportion of their lifespan than do wild-type worms, and thus have higher cognitive quality of life, while *daf-16;daf-2* mutants spend their whole lives without memory ability (**Figure 4D**).

To identify candidate genes that improve memory and slow cognitive aging in long-lived *daf-2* mutants, we compared the transcriptional profiles of Day 8 *daf-2* with Day 8 wild-type and *daf-16;daf-2* neurons, at which day wild-type and *daf-16;daf-2* worms have already lost their learning and memory ability,

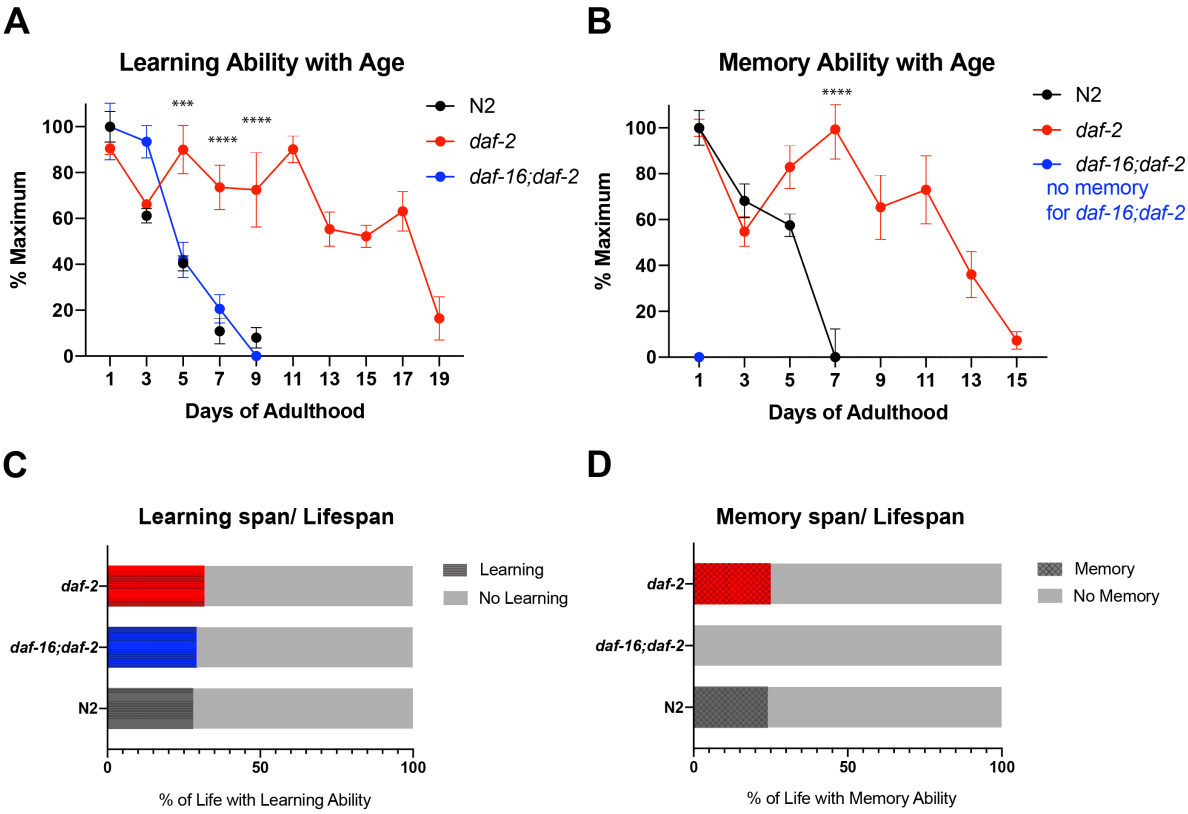

Figure 4. *daf-2* mutation improves learning and memory span compared with wild-type and *daf-16;daf-2*. (A) *daf-2* mutants show better learning maintenance with age compared to N2 and *daf-16;daf-2* worms. N = 10 plates in each condition. (B) *daf-2* mutants show better memory maintenance with age compared to N2 worms. *daf-16;daf-2* worms do not have 1hr memory on Day 1 of adulthood. N = 10 plates in each condition. (C-D) *daf-2* mutants have a larger learning span/lifespan ratio and memory span/lifespan ratio than N2 (wild type). Maximum lifespan was calculated from Tepper et al., 2013.

but *daf-2* worms still maintain most of their cognitive functions (**Figure 4A, B**). The PCA of the *daf-2*, *daf-16;daf-2*, and wild-type neuronal Day 8 transcriptomes (**Figure 5A**) indicates that *daf-16;daf-2* mutant neurons are similar to wild-type, correlating well with their similarly worsened cognitive functions at this age. Downsampling analysis shows that our sequencing depth is sufficient to saturate the detectable differential expression (**Figure S3F, S3G**). We obtained an average of 47,233,119 counted reads per sample (**Table S5**) and detected expression of 16,488 coding and non-coding genes (**Figure S3C**).

We found that about a third of the *daf-2*-upregulated genes were shared between the *daf-2* vs *daf-16;daf-2* analysis and the *daf-2* vs N2 analysis (338 genes) (**Figure 5B, Table S3, Table S4**). These shared genes are related to stress response, including heat stress (e.g., *hsp-12.6, hsp-12.3*), oxidative stress (e.g., *sod-3*), and metal stress genes (e.g., *mtl-1*). Other *daf-2*-maintained genes are specific to either the *daf-16;daf-2* comparison (proteolysis inhibitor genes, including *cpi-1*, *F29G6.1*, and *tep-1*) or to the N2 comparison (bZIP transcription factors, including *zip-5*, *zip-4*, *atf-2*, and proteasome components) (**Figure 5C,D, Figure S5D).** Over 35% of the downregulated genes are shared between the *daf-2* vs *daf-16;daf-2* set and the *daf-2* vs N2 set (**Figure S5F**). These downregulated genes are involved in synaptic transport, insulin metabolism, and chromatin structure changes during transcription. Insulin-like peptides were significantly downregulated in both *daf-2* vs N2 and *daf-2* vs *daf-16;daf-2* comparison, e.g., *ins-19*, *ins-*

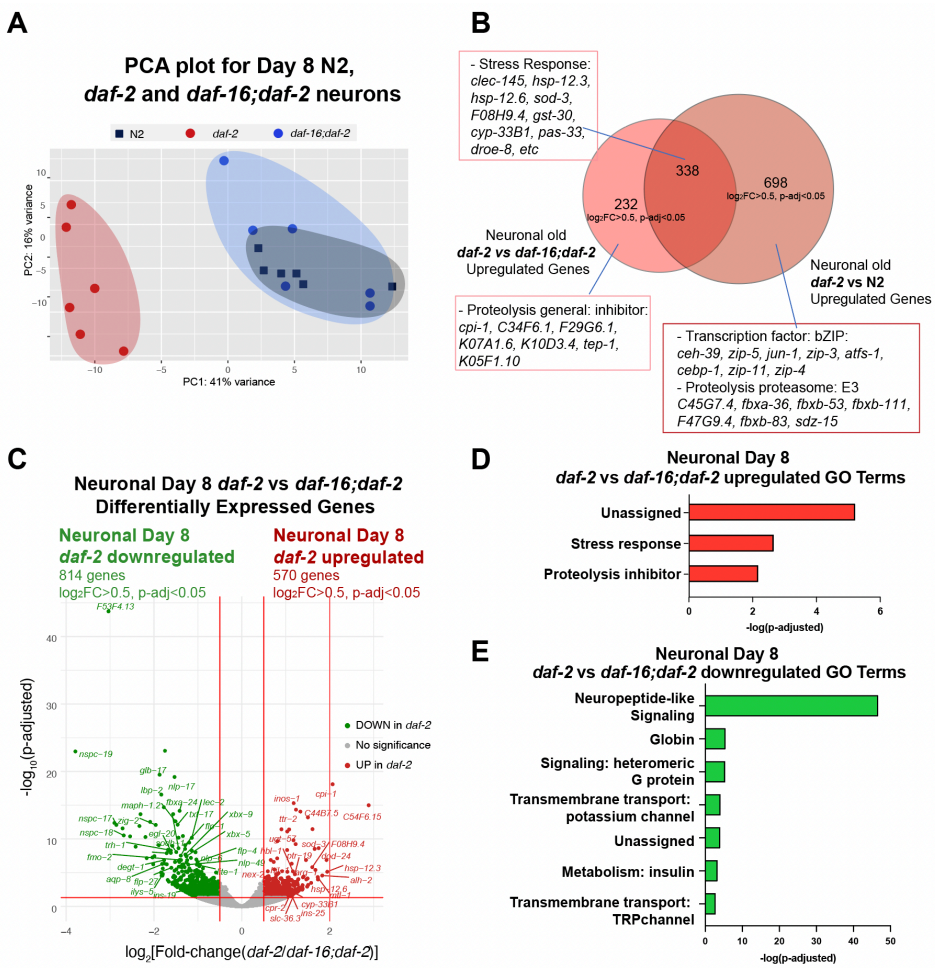

Figure 5. Identifying neuronal IIS/FOXO targets in aged worms using neuron-specific RNA-sequencing. (A) PCA plot of Day 8 N2, *daf-2,* and *daf-16;daf-2* neuronal bulk sequencing results. (B) Comparison of neuronal Day 8 DAF-16/FOXO-dependent and -independent IIS targets. Enriched GO terms and representative genes shown for each category. (C) Volcano plot of neuronal *daf-2*-regulated, *daf-16*-dependent up- (Neuronal Day 8 Class I, red) and downregulated (Neuronal Day 8 Class II, green) genes on adult Day 8 (Adjusted p-value < 0.05, $\log_2$(Fold-change) > 0.5, N = 6 biological replicates per strain). 571 genes were significantly upregulated and 814 genes were downregulated in *daf-2* neurons compared with *daf-16;daf-2.* (D) GO terms of Day 8 neuronal *daf-2* vs *daf-16-daf-2*-upregulated genes. *daf-2*-upregulated genes are related to longevity pathway, stress response, and proteolysis. (E) GO terms of Day 8 neuronal *daf-2* vs *daf-16;daf-2* downregulated genes.

9, *ins-32* (**Figure 5E**). (Note that *ins-19* expression rises with age in wild-type neurons, and its downregulation in *daf-2* neurons correlates with the improvement in memory upon its deletion in wild-type worms (**Figure 3F**). Together, the expression patterns in aged *daf-2* neurons provide us with additional candidates that could regulate neuronal activities and cognitive functions.

IIS/FOXO transcriptomic changes are necessary for *daf-2* mutant's improved neuronal functions

If the upregulated genes in aged *daf-2* neurons are responsible for the extended memory span of *daf-2* mutants, knocking down those genes should block old *daf-2* mutants' memory functions. Therefore, we tested the effect of RNAi knockdown of selected candidate genes on *daf-2's* memory on Day 6 of adulthood; at this age, wild-type worms have already lost their learning and most memory abilities, but *daf-2* worms retain normal cognitive functions. As shown

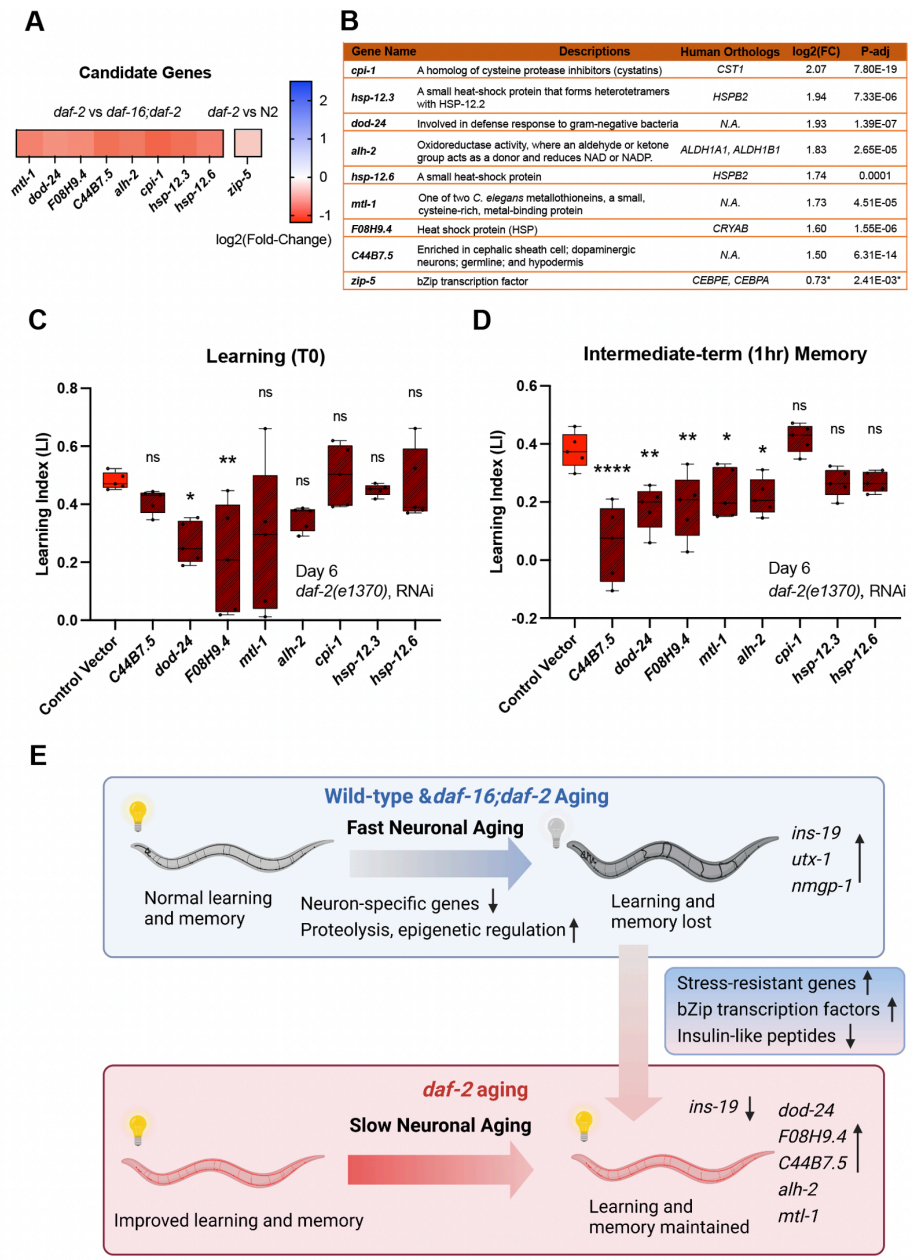

Gene Name	Descriptions	Human Orthologs	log2(FC)	P-adj
cpi-1	A homolog of cysteine protease inhibitors (cystatins)	*CST1*	2.07	7.80E-19
hsp-12.3	A small heat-shock protein that forms heterotetramers with HSP-12.2	*HSPB2*	1.94	7.33E-06
dod-24	Involved in defense response to gram-negative bacteria	*N.A.*	1.93	1.39E-07
alh-2	Oxidoreductase activity, where an aldehyde or ketone group acts as a donor and reduces NAD or NADP.	*ALDH1A1, ALDH1B1*	1.83	2.65E-05
hsp-12.6	A small heat-shock protein	*HSPB2*	1.74	0.0001
mtl-1	One of two *C. elegans* metallothioneins, a small, cysteine-rich, metal-binding protein	*N.A.*	1.73	4.51E-05
F08H9.4	Heat shock protein (HSP)	*CRYAB*	1.60	1.55E-06
C44B7.5	Enriched in cephalic sheath cell; dopaminergic neurons; germline; and hypodermis	*N.A.*	1.50	6.31E-14
zip-5	bZip transcription factor	*CEBPE, CEBPA*	0.73*	2.41E-03*

Figure 6. Neuronal IIX/FOXO aging targets regulate memory decline with age in *daf-2* worms. (A) *daf-2*-regulated Fold-change profile of candidate genes. All candidates are upregulated in *daf-2* mutants. (B) Description of candidate genes. $\log_2$(Fold-change) and p-adjusted values from the *daf-2* vs *daf-16;daf-2* comparison unless stated otherwise. *: *zip-5* is only significantly upregulated in the *daf-2* vs N2 comparison, so we are showing *daf-2* vs N2 log2(Fold-change) result here. (C) Candidate gene knockdown effects on Day 6 adult *daf-2* learning (0hr after conditioning). Two candidate genes, *dod-24* and *F08H9.4*, show a significant decrease in learning ability. N = 5 plates in each condition, representative image of 3 biological repeats shown. (D) Candidate gene knockdown effects on Day 6 adult *daf-2* short-term memory (1hr after conditioning). 5 genes show a significant decrease in memory, including *C44B7.5*, *dod-24*, *F08H9.4*, *mtl-1,* and *alh-2*. N = 5 plates in each condition, representative image of 3 biological repeats shown. *: $p < 0.05$. **: $p < 0.01$. ****: $p < 0.0001$. (E) During normal neuronal aging (wild-type and *daf-16;daf-2*), neuron-specific genes decrease in expression, while proteolysis and epigenetic regulators are upregulated, resulting in neuron morphology abnormality and cognitive function loss. *ins-19*, *utx-1,* and *nmgp-1*'s higher expression in aged animals contribute to this phenotypic change. In aged daf-2 neurons, stress-resistant genes, bZip transcription factors are upregulated, and insulin-like peptides including *ins-19* downregulated, resulting in better learning and memory maintenance with age. Upregulation of *dod-24*, *F08H9.4*, *C44B7.5*, *alh-2*, and *mtl-1* contribute to *daf-2*'s improved cognitive function.

in **Figure 6A-B**, we selected these significantly differentially-expressed candidate genes based on their ranking in fold-change; we chose genes that are significantly more highly expressed in *daf-2* mutants compared to *daf-16;daf-2* mutants (**Figure 6A**). Of the eight candidate genes we tested, the reduction of five of them significantly decreased learning (**Figure 6C**) and memory (**Figure 6D**) in Day 6 *daf-2* mutants. We found that knockdown of the heat shock-related gene *F08H9.4*, the innate immunity gene *dod-24*, the metal stress gene *mtl-1*, aldehyde dehydrogenase *alh-2* and previously uncharacterized gene *C44B7.5* are all required for *daf-2's* extended learning and memory ability. Interestingly, *mtl-1* was not found to be required for memory improvement in Day 1 *daf-2* worms (Kaletsky et al. 2016) but is required in aged *daf-2* worms. This suggests that memory maintenance with age might require additional functions not uncovered in young animals.

Since *daf-2*'s extended learning and memory depend on *daf-16*, we hypothesized that *daf-2*-upregulated, but *daf-16*-independent targets may be involved in other neuronal functions. bZip transcription factors are among the *daf-16*-independent targets in our dataset (**Figure 5B**). Previous results from our lab showed that *zip-5*, which is a bZip transcription factor upregulated in *daf-2* compared to N2 (**Figure 6A,B**), has a role in regulating axon regeneration[23]. *daf-2;zip*-5 double mutation significantly impaired *daf-2*'s ability to facilitate axon regeneration in both Day 1 (young) and Day 5 (aged) animals[23]. This indicates that *daf-2*-regulated, *daf-16*-independent targets may also elicit essential neuronal functions that promote aging and cognitive decline when lost.

Together, these data suggest that the specific genes that are differentially regulated in Day 8 *daf-2* mutants may be responsible for slowing neuronal function decline and behavioral change associated with aging.

Discussion

Here we have characterized the neuronal transcriptome of aging wild-type worms, as well as the neuronal transcriptomes of IIS (*daf-2*) and IIS/FOXO (*daf-16;daf-2*) mutants (**Figure 6E**). We found that wild-type neuronal aging is characterized by a downregulation of neuronal function genes and an upregulation of proteolysis genes and transcriptional and epigenetic regulators, which together help explain the loss of neuronal identity and function with age. We also identified the transcriptomic profile accompanying *daf-2*'s extended learning and memory span. Specifically, *daf-2* neurons maintain higher expression of stress response genes, which may make them more resistant to environmental adversities and age-related decline. We also identified genes responsible for wild-type worms' worsened learning and memory with age and genes required for maintaining *daf-2's* extended learning memory span.

By employing a FACS-based neuron-sorting technique followed by behavioral analyses, we can selectively analyze neuron-function-related genes and investigate their aging process, which is not easily discernible through whole-worm sequencing. For example, *dod-24*, which we observed to be upregulated in *daf-2* neurons and required for *daf-2*'s extended memory, is downregulated in the *daf-2* whole-worm transcriptome (**Figure S4F**). *dod-24* has been traditionally classified as a Class II gene that is downregulated in *daf-2* worms and upregulated in *daf-16* mutants and by *daf-16* RNAi treatment[10,38]. Functionally, it has been shown to be an innate immunity gene upregulated during pathogen infection[39–41], and its whole-body reduction has been shown to extend the lifespan of wild-type animals[10]. However, here we find *dod-24* is beneficial in the nervous system and is required for *daf-2*'s extended learning and memory in aged worms. This intriguing contrast between the

whole-worm transcriptome and the neuron-specific transcriptome suggests that some genes may have distinct regulatory roles in the nervous system, necessitating a more precise approach beyond whole-worm transcriptomics.

Using this neuron-specific sequencing profile on aged cells, we identified key pathways that change during neuron aging. Our sequencing of aged neurons uncovered active transcriptomic alterations during aging, resulting in not just transcriptional silencing but also upregulation of various pathways. Here, we identified age-related upregulation of histone subunits and histone modification enzymes (**Figure 2B-D**). While alterations in histone regulation are commonly observed during aging[42], our study systematically profiled neuron-specific upregulation of epigenetic genes, and our behavioral results of *utx-1* further suggest that addressing this epigenetic dysregulation may have beneficial implications for cognitive behaviors.

We also identified Day 8 neuronal *daf-2* vs *daf-16;daf-2* differentially expressed genes that are different compared to the Day 1 list[15]. While the neuronal Day 1 *daf-2*-upregulated genes emphasize neuron-specific targets, on Day 8, there were fewer neuron-specific candidates (**Figure S4E**). However, the list became more like the whole-worm list (30% overlap, **Figure S4F**), suggesting that both wild-type and *daf-2* neurons experience a gradual loss of neuronal identity with age. These changes suggest that *daf-2*'s extended memory maintenance may require different mechanisms; *daf-2* may maintain neuronal function not just by retaining a youthful transcriptome, but also by increasing the expression of genes that promote resilience, such as stress-response genes and proteolysis inhibitors.

Sequencing many biological repeats of aging neurons to high depth, and sequencing total RNA with ribosomal RNA depletion (**Table S5**), allowed us to detect a larger number of genes compared to other neuron-related bulk and single-cell sequencing profiles, providing a deep transcriptomic dataset of aged wild-type, IIS mutant, and IIS/FOXO mutant neurons. Our analysis allowed us to identify several differentially-expressed genes that are known to be expressed in at a small number of neurons, even for low-abundance genes. Notably, our sequencing results uncovered genes previously not shown to be expressed in the neurons in other datasets, including *sup-6*, *cey-2, his-64,* and *adk-1* (**Figure S6**). Moreover, this analysis revealed the involvement of known neuronal genes in the aging process, such as *ins-6* and *srd-23*. We hope that this dataset will become a valuable resource for detecting new candidates in neuronal aging.

In addition to examining aging in wild-type and IIS/FOXO mutants independently, our results further linked the normal aging process to altered gene regulation in the IIS pathway. *utx-1* is an H3K27me3 histone demethylase we found to be higher in wild-type aged neurons, but it is also involved in the IIS pathway. The downregulation of *utx-1* has been shown to regulate development[30] and promote longevity[31–33], and its mammalian homolog has been implicated in regulating cognitive abilities[34,35]. The longevity response of *utx-1* depends on *daf-16*[31–33]. The loss of *utx-1* decreases methylation on the *daf-2* gene, thus increasing DAF-16's nuclear localization, mimicking a *daf-2* mutation[31]. This example of the crosstalk between normal aging and IIS/FOXO mutants offers valuable insights into modifying the aging process for enhanced longevity and cognitive health.

We found that the insulin-like peptide *ins-19* was upregulated in aged neurons and was downregulated in aged *daf-2* neurons, and its downregulation in wild-type worms extended memory span. Insulin-like peptides play crucial roles as receptor ligands (in both

agonist and antagonist roles) for DAF-2, and we have found them to be downregulated in *daf-2* mutants compared with *daf-16;daf-2* mutants, possibly creating a feedback loop that dampens the insulin signaling pathway, as was previously shown for *ins-7* and *ins-18*[10,43]. These peptides exhibit diverse functions in development, dauer formation, and longevity[10,43–47]. Notably, certain insulin-like peptides have been linked to neuronal activities, such as the regulation of aversive learning by the two antagonistic peptides *ins-6* and *ins-7*[28], and reduced long-term learning and memory by *ins-22* RNAi[48]. In our study, the expression changes of *ins-19* during wild-type aging and in *daf-2* mutants provide an example of how longevity mutants can reverse wild-type transcriptional changes during aging, ultimately reducing behavioral and functional decline.

Beyond our sequencing analysis, we have established links between genomics, function, and behavior. *utx-1, nmgp-1,* and *ins-19* increase in expression in aged neurons, and we found that their reduction improved memory, indicating genes whose expression rises with age can have a negative impact on normal cognitive functions. We also identified several new genes required for *daf-2*'s age-related improvement in learning and memory - namely *dod-24*, *F08H9.4*, *C44B7.5*, *alh-2,* and *mtl-1* - shedding light on their neuron-specific roles. These additional findings further suggest that these neuronal sequencing datasets can be used to identify functional candidates and pathways during the aging process. By bridging the gap between transcriptomic landscapes, genetic regulation, and functional outcomes, our study provides a greater understanding of the mechanisms underlying neuronal aging and may help with development of aging interventions and therapeutics.

Conclusions

We sequenced wild-type aging neurons and IIS/FOXO longevity mutant neurons, leading to the identification of crucial pathways that undergo changes during aging. Additionally, our dataset will serve as a comprehensive and reliable resource for the field of aging, with a particular focus on neuron-specific genes and pathways. Moreover, we established connections between the normal aging process and *daf-2*-regulated longevity mutants, providing insights into the regulation of aging and the promotion of cognitive health. Lastly, we validated the sequencing results by conducting imaging and behavioral experiments on candidate genes implicated in age-related cognitive decline, effectively transforming expression level correlations into causal behavioral outcomes, advancing our knowledge of age-related cognitive decline regulation.

Acknowledgements

We thank the *Caenorhabditis* Genetics Center (CGC) for strains, WormBase (version WS289) for information, Jasmine Ashraf, William Keyes, Yichen Weng, and Titas Sengupta for help with experiments, members of the Murphy Lab for input on the manuscript, Christina DeCoste, Katherine Rittenbach and the Flow Cytometry Facility for cell sorting assistance, Wei Wang and the Genomics Facility for sequencing assistance, Lance Parsons, Bruce Wang, and Chen Dan for insights on data analysis, and Biorender.com for schematic design. C.T.M. is the Director of the Simons Collaboration on Plasticity in the Aging Brain (SCPAB), which supported the work, and the Glenn Center for Aging Research at Princeton. Y.W. and S.Z. are supported by China Scholarship Council (CSC). K.M. is supported by HHMI Gilliam Fellows Program.

Author Contributions

C.T.M., R.K., S.Z., and Y.W. conceived and designed experiments. Y.W. and S.Z. performed RNA-sequencing experiments. Y.W., S.Z., and K.M. performed behavioral assays.

Y.W. performed imaging experiments. Y.W., S.Z., K.M., S.L., R.K., and C.T.M. analyzed and interpreted results. Y.W. and C.T.M wrote the paper.

Methods

Resource availability

Further information and requests for resources and reagents should be directed to and will be fulfilled by Coleen T. Murphy (ctmurphy@princeton.edu).

Data availability

Sequencing reads are deposited at NCBI BioProject under accession number PRJNA999305.

Code availability

Analysis codes generated from this study are available upon request.

C. elegans strains and cultivation

N2 (wild type),
OH441: otIs45(*unc-119::GFP*),
CQ295: otIs45(*unc-119::GFP*);*daf-2(e1370)*,
CQ296: otIs45(*unc-119::GFP*) ;*daf-16(mu86);daf-2(e1370)*,
LC108: uIs69 (*myo-2p::mCherry + unc-119p::sid-1*),
CQ705: daf-2(e1370) III, 3X outcrossed,
CQ745: *daf-2(e1370) III;* vIs69 [*pCFJ90(Pmyo-2::mCherry + Punc-119::sid-1)*] *V*, QL188: *ins-19(tm5155) II*,
CX3695: kyIs140(*str-2::GFP + lin-15(+)*),
CQ461*: (daf-2(e1370);Pmec-4::mCherry)*
CQ501*: (daf-2 (e1370);zip-5(gk646);Pmec-4::mCherry)*. Strains were grown on high-growth media (HGM) plates seeded with E. coli OP50 bacteria using standard methods [49]. For neuronal isolations, worms were synchronized by hypochlorite treatment, eggs spread on seeded plates to hatch and grown to L4 on HGM plates until transferred to HGM plates with FUdR to avoid progeny contamination.

Tissue-specific FACS

Neuron isolation and Fluorescent-activated cell sorting were carried out as previously described [15,50]. Briefly, worms were treated with 1000uL lysis buffer (200 mM DTT, 0.25% SDS, 20 mM HEPES pH 8.0, 3% sucrose) for 6.5 mins to break the cuticle. Worms were washed and resuspended in 500uL 20mg/mL pronase from *Streptomyces griseus* (Sigma-Aldrich). Worms were incubated at room temperature with mechanical disruption by pipetting until no whole-worm bodies were seen, and then ice-cold osmolarity adjusted L-15 buffer (Gibco) with 2% Fetal Bovine Serum (Gibco) were added to stop the reaction. Prior to sorting, cell suspensions were filtered using a 5um filter and sorted using a FACSVantage SE w/ DiVa (BD Biosciences; 488nm excitation, 530/30nm bandpass filter for GFP detection). Sorting gates were determined by comparing with age-matched, genotype-matched non-fluorescent cell suspension samples. Fluorescent neuron cells were directly sorted into Trizol LS. 100,000 GFP+ cells were collected for each sample.

RNA extraction, library generation and sequencing

We used standard trizol-chloroform-iso-propanol method to extract RNA, then performed RNA cleanup using RNeasy MinElute Cleanup Kit (Qiagen). RNA quality was assessed using the Agilent Bioanalyzer RNA Pico chip, and bioanalyzer RIN>6.0 samples were observed before library generation. 2ng of RNA was used for library generation using Ovation SoLo RNA-Seq library preparation kit with AnyDeplete Probe Mix- *C. elegans* (Tecan Genomics) according to the manufacturer's instructions[51]. Library quality and concentration was assessed using Agilent Bioanalyzer DNA 12000 chip. Samples were multiplexed and sequencing were performed using NovaSeq S1 100nt Flowcell v1.5 (Illumina).

Data processing

FastQC was performed on each sample for quality control analysis. RNA STAR package was used for mapping paired-end reads to the *C. elegans* genome ce11 (UCSC Feb 2013) using the gene model ws245genes.gtf. Length of the genomic sequence around annotated junctions is chosen as read length - 1. 50-70% reads were uniquely mapped. Reads uniquely mapped to the genome were then counted using htseq-count (mode = union). DESeq2 analysis was then used for read normalization and differential expression analysis on counted reads [52]. Genes with a $\log_{10}$TPM >0.5 were considered as detected and genes with a $\log_2$(fold-change) > 0.5 and p-adjusted <0.05 are considered differentially expressed in further analysis. Gene ontology analysis were performed using gprofiler[53] or WormCat 2.0[54] and category 2 was selected to show. Tissue query was performed on top 500 highest fold-change genes, using worm tissue query website (www.worm.princeton.edu)[50], and only major systems were selected in the analysis.

Learning and Memory Experiments

We performed Short-Term Associative Memory (STAM) experiments as previously described[7,55]. Briefly, we performed chemotaxis assays to butanone on naïve and appetitive-trained worms at different time points to assess change in preference to butanone. Chemotaxis index is calculated using this function: (# of worms at butanone- # of worms at ethanol)/(total # of worms - # of worms at origin). Learning index is calculated by subtracting trained chemotaxis index with naïve chemotaxis index.

For learning and memory span assays, we obtained synchronized worms from hypochlorite-treated eggs. Synchronized worms were washed onto 5'-fluorodeoxyuridine (FUdR) at L4 and maintained on FUdR plates by transferring to new plates every 2 days. 1 Day Prior to experiments, worms are washed onto fresh HG plates without FUdR to avoid change in behavior caused by FUdR. For *utx-1* and *nmgp-1* RNAi experiments, synchronized L4 worms were washed onto HGM plates with carbenicillin and IPTG and seeded with HT115 RNAi bacteria containing the RNAi constructs from the Ahringer Library. For *daf-2* upregulated candidates' RNAi experiments, synchronized L4 worms were washed onto HGM plates added with carbenicillin, FUdR and iso-propyl-b-D-thiogalactopyranoside (IPTG) and seeded with HT115 bacteria containing RNAi constructs generated from Ahringer RNAi Library, and transferred onto frish RNAi plates every 2 days until Day 6. 1 Day Prior to experiments, worms are transferred onto plates without FUdR.

Neuron Morphology

We transferred synchronized worms to FUdR at L4 and maintained by transferring them to fresh plates every 2 days. We imaged worms on adult Day 2 and Day 12, using Nikon AXR confocal microscope's GFP channel at 60X magnification and 0.5um Z-stack. Images were processed using NIS-Elements and FIJI software, and blindly quantified. Beading was measured as bead-like varicosities in the neurite, and deviation was measured as significant path changes from normal neurite processes. Imaging was performed in 3 biological replicates, and 40 Day 2 and 56 Day 12 worms were imaged. Data analysis was performed using Prism software, and Chi-square statistical measurements were used.

Quantitative and Statistical Analysis

All experimental analysis was performed using Prism 8 software. Two-way ANOVA with Tukey post-hoc tests were used to compare the learning curve between control and experimental groups. One-way ANOVA

followed by Dunnet post-hoc tests for multiple comparisons was performed to compare learning or 2hr memory between various treatment groups and control. Chi-square test was performed to compare the neuron morphology change between young and aged AWC neurons. All GO term analysis were perform using Wormcat 2.0 software with Bonferroni corrected adjusted p-values. Venn diagram overlaps were compared using the hypergeometric test. Differential expression analysis of RNA-seq were performed using DESeq2 algorithm and adjusted p-values were generated with Wald test using Benjamini and Hochberg method (BH-adjusted p values). Additional statistical details of experiments, including sample size (with n representing the number of chemotaxis assays performed for behavior, RNA collections for RNA-seq, and the number of worms for microscopy), can be found in the methods and figure legends.

References

1. Plassman, B. L. *et al.* Prevalence of cognitive impairment without dementia in the United States. *Ann. Intern. Med.* **148**, 427–434 (2008).
2. Langa, K. M. & Levine, D. A. The diagnosis and management of mild cognitive impairment: a clinical review. *JAMA* **312**, 2551–2561 (2014).
3. Gillis, C., Mirzaei, F., Potashman, M., Ikram, M. A. & Maserejian, N. The incidence of mild cognitive impairment: A systematic review and data synthesis. *Alzheimers Dement. Diagn. Assess. Dis. Monit.* **11**, 248–256 (2019).
4. Feigin, V. L. *et al.* The global burden of neurological disorders: translating evidence into policy. *Lancet Neurol.* **19**, 255–265 (2020).
5. Nichols, E. & Vos, T. Estimating the global mortality from Alzheimer's disease and other dementias: A new method and results from the Global Burden of Disease study 2019. *Alzheimers Dement.* **16**, e042236 (2020).
6. White, J., Southgate, E., Thomson, J. & Brenner, S. The structure of the nervous system of the nematode Caenorhabditis elegans. *Philos. Trans. R. Soc. Lond. B. Biol. Sci.* **314**, 1–340 (1986).
7. Kauffman, A. L., Ashraf, J. M., Corces-Zimmerman, M. R., Landis, J. N. & Murphy, C. T. Insulin Signaling and Dietary Restriction Differentially Influence the Decline of Learning and Memory with Age. *PLoS Biol.* **8**, e1000372 (2010).
8. Arey, R. N. & Murphy, C. T. Conserved regulators of cognitive aging: From worms to humans. *Behav. Brain Res.* **322**, 299–310 (2017).
9. Kenyon, C., Chang, J., Gensch, E., Rudner, A. & Tabtiang, R. A C. elegans mutant that lives twice as long as wild type. *Nature* **366**, 461–464 (1993).
10. Murphy, C. T. *et al.* Genes that act downstream of DAF-16 to influence the lifespan of Caenorhabditis elegans. *Nature* **424**, 277–284 (2003).
11. Clancy, D. J. *et al.* Extension of life-span by loss of CHICO, a Drosophila insulin receptor substrate protein. *Science* **292**, 104–106 (2001).
12. Blüher, M., Kahn, B. B. & Kahn, C. R. Extended longevity in mice lacking the insulin receptor in adipose tissue. *Science* **299**, 572–574 (2003).
13. Suh, Y. *et al.* Functionally significant insulin-like growth factor I receptor mutations in centenarians. *Proc. Natl. Acad. Sci. U. S. A.* **105**, 3438–3442 (2008).
14. Willcox, B. J. *et al.* FOXO3A genotype is strongly associated with human longevity. *Proc. Natl. Acad. Sci. U. S. A.* **105**, 13987–13992 (2008).
15. Kaletsky, R. *et al.* The C. elegans adult neuronal IIS/FOXO transcriptome reveals adult phenotype regulators. *Nature* **529**, 92–96 (2016).
16. Hahm, J. H. *et al.* C. elegans maximum velocity correlates with healthspan and is maintained in worms with an insulin receptor mutation. *Nat. Commun.* **6**, 1–7 (2015).

17. Liu, J. *et al.* Functional aging in the nervous system contributes to age-dependent motor activity decline in C. elegans. *Cell Metab.* **18**, 392–402 (2013).
18. Li, L. B. *et al.* The Neuronal Kinesin UNC-104/KIF1A Is a Key Regulator of Synaptic Aging and Insulin Signaling-Regulated Memory. *Curr. Biol. CB* **26**, 605–615 (2016).
19. Pan, C. L., Peng, C. Y., Chen, C. H. & McIntire, S. Genetic analysis of age-dependent defects of the Caenorhabditis elegans touch receptor neurons. *Proc. Natl. Acad. Sci. U. S. A.* **108**, 9274–9279 (2011).
20. Tank, E. M. H., Rodgers, K. E. & Kenyon, C. Spontaneous Age-Related Neurite Branching in Caenorhabditis elegans. *J. Neurosci.* **31**, 9279–9288 (2011).
21. Toth, M. L. *et al.* Neurite Sprouting and Synapse Deterioration in the Aging Caenorhabditis elegans Nervous System. *J. Neurosci.* **32**, 8778–8790 (2012).
22. Byrne, A. B. *et al.* Insulin/IGF1 Signaling Inhibits Age-Dependent Axon Regeneration. *Neuron* **81**, 561–573 (2014).
23. Lakhina, V. *et al.* ZIP-5/bZIP transcription factor regulation of folate metabolism is critical for aging axon regeneration. *bioRxiv* 727719 (2019) doi:10.1101/727719.
24. Torayama, I., Ishihara, T. & Katsura, I. Caenorhabditis elegans Integrates the Signals of Butanone and Food to Enhance Chemotaxis to Butanone. *J. Neurosci.* **27**, 741–750 (2007).
25. Robinson, D. G. & Storey, J. D. subSeq: Determining Appropriate Sequencing Depth Through Efficient Read Subsampling. *Bioinformatics* **30**, 3424–3426 (2014).
26. Taylor, S. R. *et al.* Molecular topography of an entire nervous system. *Cell* **184**, 4329-4347.e23 (2021).
27. Artan, M. *et al.* Food-derived sensory cues modulate longevity via distinct neuroendocrine insulin-like peptides. *Genes Dev.* **30**, 1047–1057 (2016).
28. Chen, Z. *et al.* Two insulin-like peptides antagonistically regulate aversive olfactory learning in C. elegans. *Neuron* **77**, 572–585 (2013).
29. Brear, A. G., Yoon, J., Wojtyniak, M. & Sengupta, P. Diverse cell type-specific mechanisms localize G protein-coupled receptors to Caenorhabditis elegans sensory cilia. *Genetics* **197**, 667–684 (2014).
30. Vandamme, J. *et al.* The C. elegans H3K27 Demethylase UTX-1 Is Essential for Normal Development, Independent of Its Enzymatic Activity. *PLOS Genet.* **8**, e1002647 (2012).
31. Jin, C. *et al.* Histone demethylase UTX-1 regulates C. elegans life span by targeting the insulin/IGF-1 signaling pathway. *Cell Metab.* **14**, 161–172 (2011).
32. Maures, T. J., Greer, E. L., Hauswirth, A. G. & Brunet, A. The H3K27 demethylase UTX-1 regulates C. elegans lifespan in a germline-independent, insulin-dependent manner. *Aging Cell* **10**, 980–990 (2011).
33. Guillermo, A. R. R. *et al.* H3K27 modifiers regulate lifespan in C. elegans in a context-dependent manner. *BMC Biol.* **19**, 59 (2021).
34. Shaw, C. K. *et al.* X Chromosome Factor Kdm6a Enhances Cognition Independent of Its Demethylase Function in the Aging XY Male Brain. *J. Gerontol. A. Biol. Sci. Med. Sci.* **78**, 938–943 (2023).
35. Tang, G.-B. *et al.* The Histone H3K27 Demethylase UTX Regulates Synaptic Plasticity and Cognitive Behaviors in Mice. *Front. Mol. Neurosci.* **10**, (2017).
36. Fernández, E. M. *et al.* Neuronal membrane glycoprotein (nmgp-1) gene deficiency affects chemosensation-related behaviors, dauer exit and egg-laying in Caenorhabditis elegans. *J. Neurochem.* **160**, 234–255 (2022).
37. Bansal, A., Zhu, L. J., Yen, K. & Tissenbaum, H. A. Uncoupling lifespan and healthspan in caenorhabditis elegans longevity mutants. *Proc. Natl. Acad. Sci. U. S. A.* **112**, E277–E286 (2015).
38. Tepper, R. G. *et al.* PQM-1 complements DAF-16 as a key transcriptional regulator of DAF-2-mediated development and longevity. *Cell* **154**, 676–690 (2013).
39. Shapira, M. *et al.* A conserved role for a GATA transcription factor in regulating epithelial innate immune responses. *Proc. Natl. Acad. Sci.* **103**, 14086–14091 (2006).
40. Eckl, J., Sima, S., Marcus, K., Lindemann, C. & Richter, K. Hsp90-downregulation influences the heat-shock response, innate immune response and onset of oocyte development in nematodes. *PloS One* **12**,

(2017).
41. Mack, H. I. D., Kremer, J., Albertini, E., Mack, E. K. M. & Jansen-Dürr, P. Regulation of fatty acid desaturase- and immunity gene-expression by mbk-1/DYRK1A in Caenorhabditis elegans. *BMC Genomics* **23**, (2022).
42. Yi, S.-J. & Kim, K. New Insights into the Role of Histone Changes in Aging. *Int. J. Mol. Sci.* **21**, 8241 (2020).
43. Murphy, C. T., Lee, S.-J. & Kenyon, C. Tissue entrainment by feedback regulation of insulin gene expression in the endoderm of Caenorhabditis elegans. *Proc. Natl. Acad. Sci.* **104**, 19046–19050 (2007).
44. Thomé-Duret, V. *et al.* Continuous glucose monitoring in the free-moving rat. *Metabolism* **47**, 799–803 (1998).
45. Kawano, T. *et al.* Molecular Cloning and Characterization of a New Insulin/IGF-like Peptide of the Nematode Caenorhabditis elegans. *Biochem. Biophys. Res. Commun.* **273**, 431–436 (2000).
46. Pierce, S. B. *et al.* Regulation of DAF-2 receptor signaling by human insulin and ins-1, a member of the unusually large and diverse C. elegans insulin gene family. *Genes Dev.* **15**, 672–686 (2001).
47. Li, W., Kennedy, S. G. & Ruvkun, G. daf-28 encodes a C. elegans insulin superfamily member that is regulated by environmental cues and acts in the DAF-2 signaling pathway. *Genes Dev.* **17**, 844–858 (2003).
48. Lakhina, V. *et al.* Genome-wide functional analysis of CREB/long-term memory-dependent transcription reveals distinct basal and memory gene expression programs. *Neuron* **85**, 330–345 (2015).
49. Brenner, S. THE GENETICS OF CAENORHABDITIS ELEGANS. *Genetics* **77**, (1974).
50. Kaletsky, R. *et al.* Transcriptome analysis of adult Caenorhabditis elegans cells reveals tissue-specific gene and isoform expression. *PLoS Genet.* **14**, (2018).
51. Barrett, A. *et al.* A head-to-head comparison of ribodepletion and polyA selection approaches for Caenorhabditis elegans low input RNA-sequencing libraries. *G3 GenesGenomesGenetics* **11**, (2021).
52. Love, M. I., Huber, W. & Anders, S. Moderated estimation of fold change and dispersion for RNA-seq data with DESeq2. *Genome Biol.* **15**, 550 (2014).
53. Raudvere, U. *et al.* g:Profiler: a web server for functional enrichment analysis and conversions of gene lists (2019 update). *Nucleic Acids Res.* **47**, W191–W198 (2019).
54. Holdorf, A. D. *et al.* WormCat: An online tool for annotation and visualization of caenorhabditis elegans genome-scale data. *Genetics* **214**, 279–294 (2020).
55. Kauffman, A. *et al.* C. elegans positive butanone learning, short-term, and long-term associative memory assays. *J. Vis. Exp.* 1–9 (2011) doi:10.3791/2490.

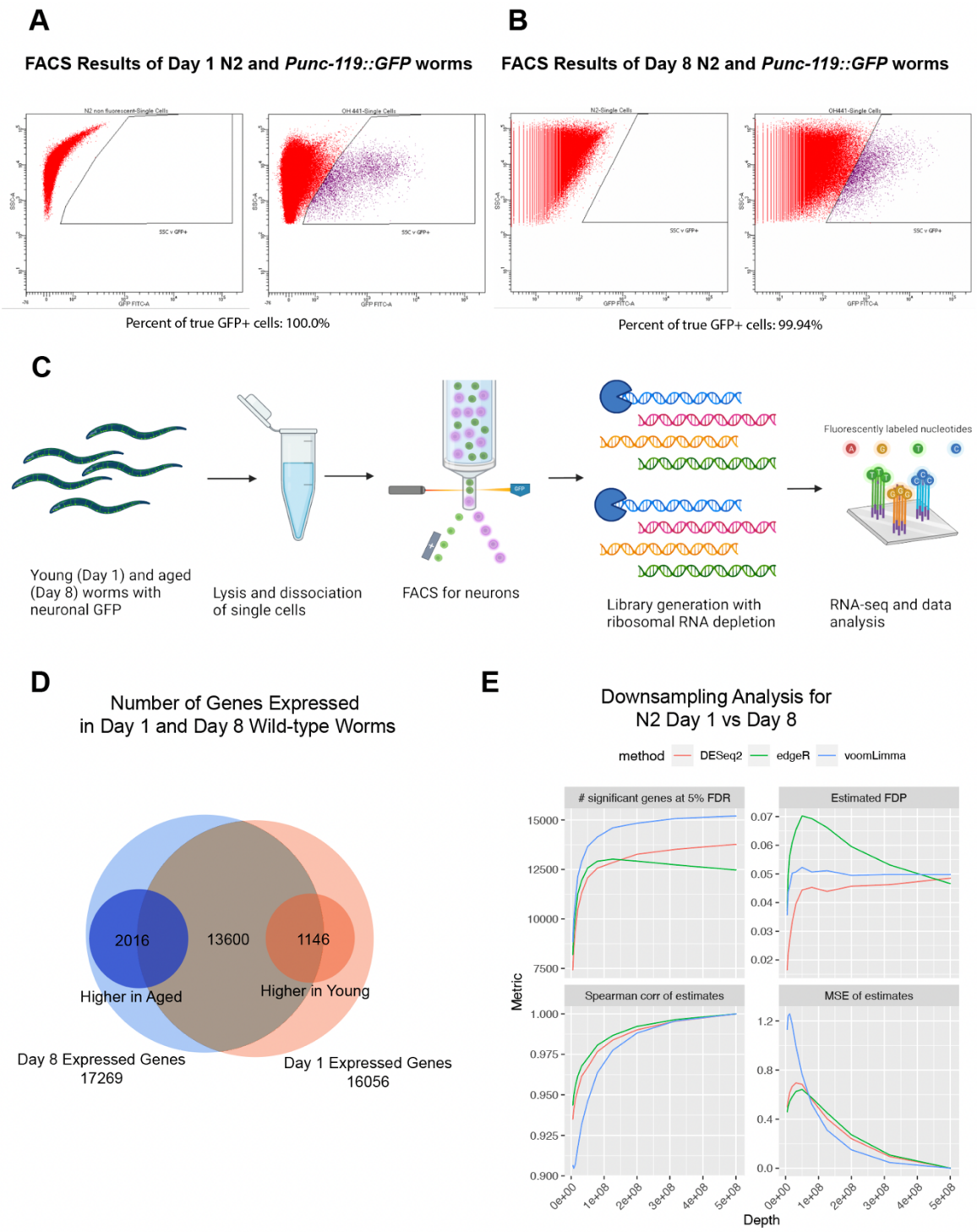

Figure S1. Aged neuron-specific sequencing. (A-B) FACS results of neuron isolation. Over 99.94% of the cells collected are GFP+ neurons. 100,000 cells are collected for each biological replicate, 6 biological replicates for each condition. (C) Workflow of neuron isolation, library generation and sequencing. (D) Number of genes detected in Day 1 and Day 8 wild-type neurons. Genes with log2(TPM)>0.5 are considered expressed. (E) Down-sampling analysis for N2 Day 1 vs Day 8 indicate downsampling 30% of the data will still yield good results, indicating sufficiency of sequencing depth.

Figure S2. Whole-worm RNA-sequencing identifies whole-body changes during aging. (A) Volcano plot of Day 1 vs Day 8 differentially-expressed genes during aging. 264 genes are expressed at higher levels in young worms, 1626 genes are higher in aged worms ($\log_2$[Fold-change(Day 1/Day 8)] >2.0, p-adjusted <0.001). (B) GO terms of genes that are expressed at higher levels in young (wild-type) whole animals highlight collagen and metabolism. (C) GO terms of genes that are expressed at higher levels in aged (wild-type) whole animals. GO terms generated using Wormcat 2.0. (D) Tissue query for whole-worm aged-related genes highlights the alimentary system. (E) Full image of comparison of top wild-type neuronal and whole-worm differentially expressed with age genes. Related to Figure 2D.

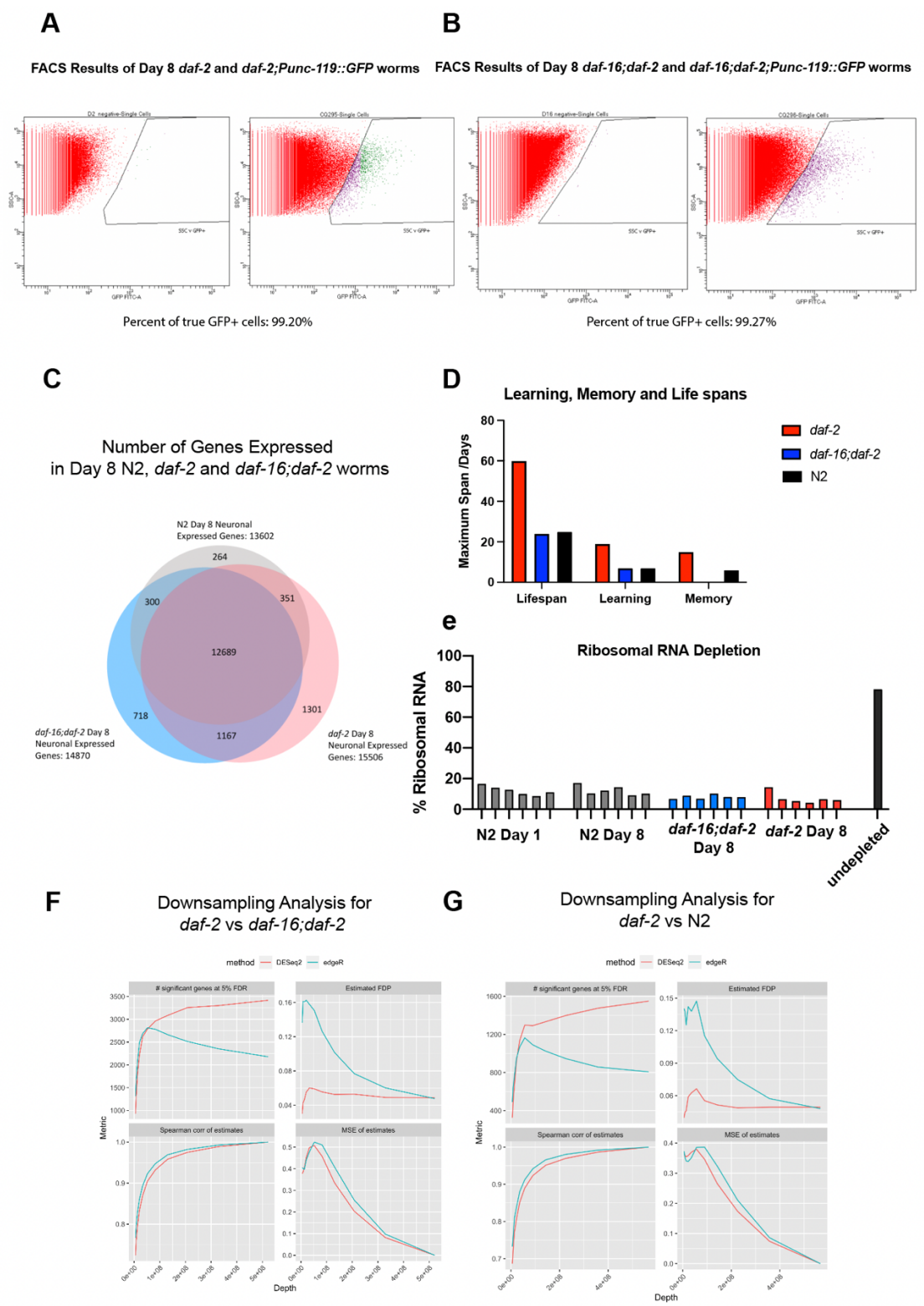

Figure S3. Neuron-specific sequencing of Day 8 *daf-2* and *daf-16;daf-2* mutants. (A-B) FACS results of neuron isolation. Over 99% of the cells collected are GFP+ neurons. 100,000 cells are collected for each biological replicate, 6 replicates for each genotype. (C) Number of genes detected in Day 8 N2, *daf-2,* and *daf-16;daf-2* neurons. (D) Number graph of lifespan, learning, and memory function. Related to Figure 4C and 4D. (E) Ribosomal RNA depletion during sequencing. We used the library generation protocol with *C. elegans*-specific ribosomal RNA depletion kit (Tecan Genomics) successfully depleted rRNA to less than 20% of total reads. (F-G) Downsampling analysis for daf-2 vs *daf-16;daf-2* and daf-2 vs N2. Both shows sufficient depth.

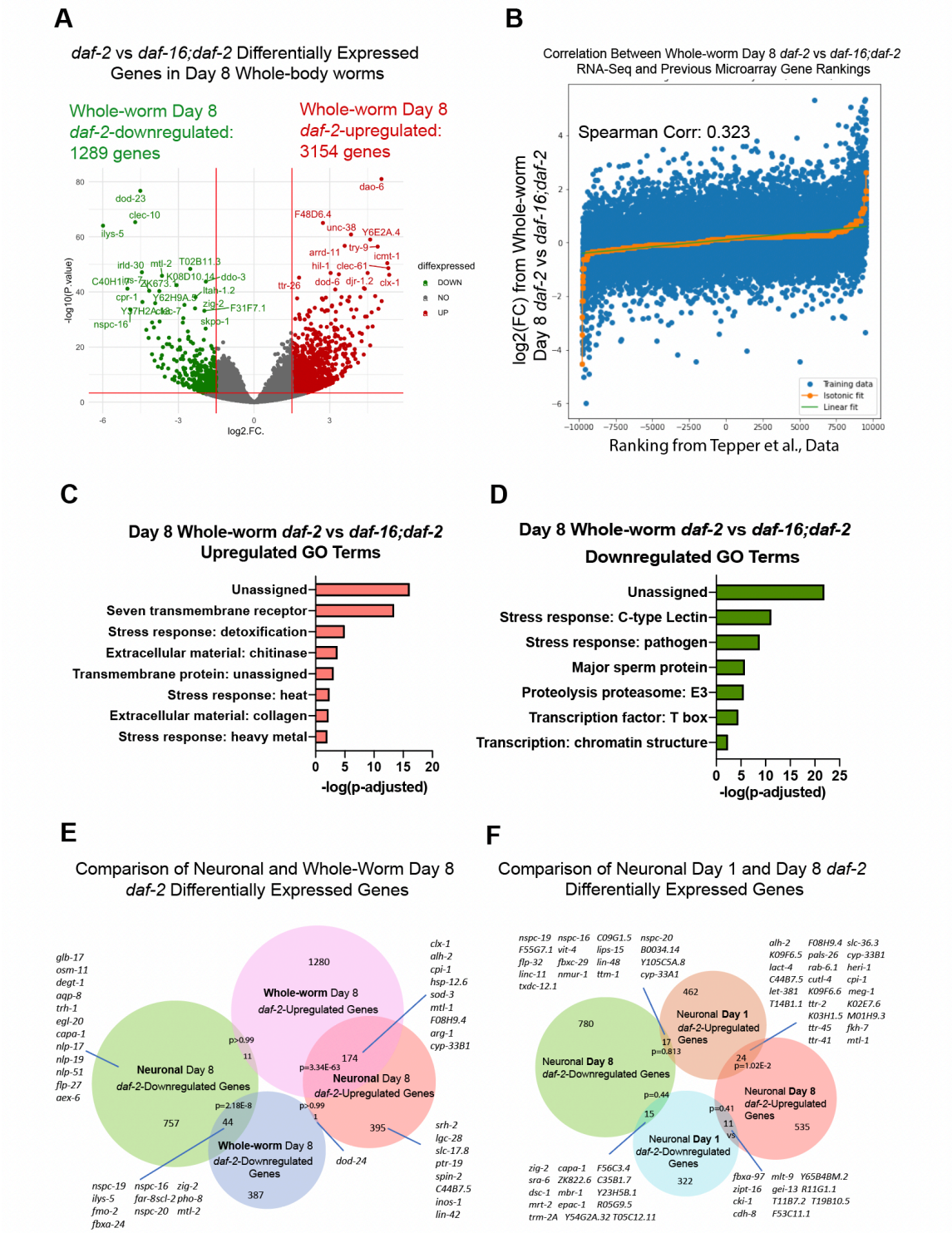

Figure S4. Whole-worm RNA-sequencing identifies changes in aged *daf-2* mutants. (A) Volcano plot of whole-worm *daf-2* vs *daf-16;daf-2* differentially expressed genes during aging. 3154 genes are higher in daf-2, 1289 genes are higher in daf-16;daf-2 ($\log_2$[Fold-change(*daf-2* vs *daf-16;daf-2*)] >1.5, p-adjusted <0.01). (B) Correlation between our whole-worm Day 8 *daf-2* and *daf-16;daf-2* sequencing and Class I and Class II gene rank from Tepper et al., 2013[38]. High correlation indicates consistency between our RNA-sequencing results with former microarray results, despite the differences in approaches and ages. Spearman correlation calculated using the SciPy package. (C-D) GO term analysis of whole-worm *daf-2*-regulated genes shows enrichment in stress-resistant genes. (E) Comparison of neuronal and whole-worm Day 8 *daf-2* differentially-expressed genes show high overlap (~30%), but also identify genes specific to neurons and to the whole body. (F) Comparison of neuronal Day 1 and Day 8 *daf-2* differentially expressed genes identifies a set of consistent and sets of changed genes.

Figure S5. DAF-16-dependent and -independent *daf-2* regulated genes show different features. (A) Tissue query for *daf-2* vs *daf-16;daf-2* differentially expressed genes. (B) Tissue query for *daf-2* vs N2 differentially expressed genes. (C) Volcano plot of *daf-2* vs N2 differentially expressed genes during aging. 1036 genes are more highly expressed in *daf-2* mutants, 1285 genes are higher in N2 ($\log_2$[Fold-change(*daf-2* vs N2)] >0.5, p-adjusted <0.05). (D-E) Neuronal Day 8 *daf-2* vs N2 differentially expressed GO Terms. (F) Full image of comparison of neuronal Day 8 *daf-2* vs *daf-16;daf-2* and *daf-2* vs N2 differentially expressed genes. Related to Figure 5B.

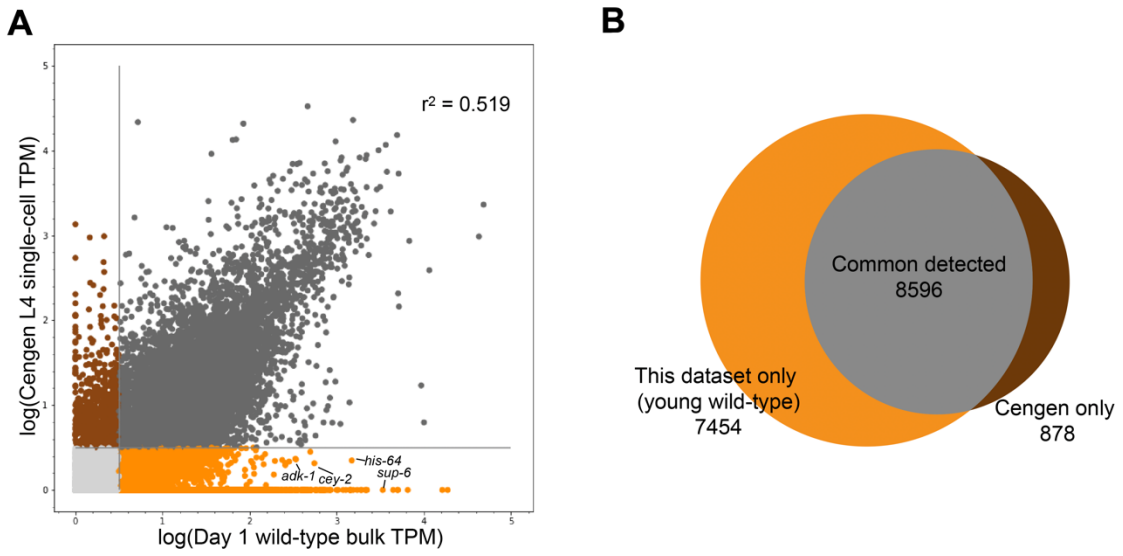

Figure S6. Comparison with recent sequencing datasets. (A) Comparison with Cengen gene expression data shows high correlation, with a lot of genes only detected in our bulk-sequencing dataset (orange). Using only the wild-type Day 1 neuron sequencing data in the comparison. Genes with an average log2(TPM) > 0.5 are considered detected. Linear regression correlation calculated using the SciPy package. (B) Venn diagram showing genes detected in this dataset (orange), Cengen dataset (brown) and both (gray). Using only wild-type Day 1 neuron sequencing data in the comparison.